NJC

New Journal of Chemistry

A journal for new directions in chemistry

Accepted Manuscript

This article can be cited before page numbers have been issued, to do this please use: P. SALUNKHE, A. A. Ghanwat, Y. Patil, I. A. Dhole, B. Kalshetti, S. R. Mane and V. Patil, *New J. Chem.*, 2019, DOI: 10.1039/C9NJ02877C.

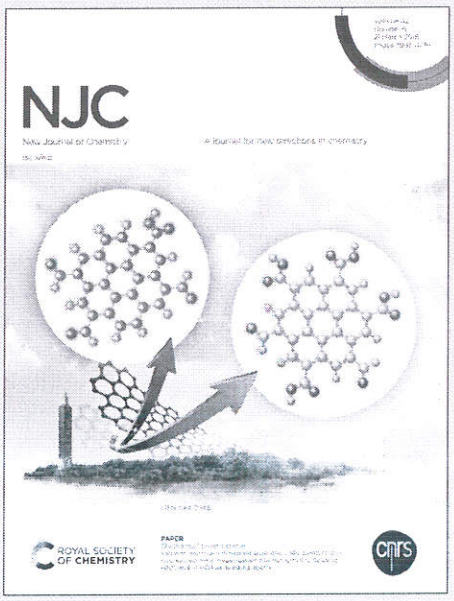

View Article Online
DOI: 10.1039/C9NJ02877C

Novel synthetic approach for designing metal free, redox active quinoxaline-benzimidazole based organic polymers with high energy storage capacity.

Pravin S. Salunkhe,[a,c] *Yuvraj S. Patil,*[a] *Indrajeet A. Dhole,*[b] *Basavraj S. Kalshetti,*[a] *Vikas B. Patil,*[b] *Shivshankar R. Mane,*[c] *and Anil A. Ghanwat*[a*]

a. Polymer Research Laboratory, School of Chemical Sciences, Solapur University, Solapur-413255, (MS), India.

b. Functional Materials Research Laboratory, School of Physical Sciences, Solapur University, Solapur-413255, (MS), India.

c. Polymer Science and Engineering Division, CSIR-National Chemical Laboratory, Pune

E-mail : **anil_ghanwat@yahoo.com**

ph.salunkhe@ncl.res.in

Graphical Abstract:

We established the first use of thiophene integrated with quinoxaline-benzimidazole unit for energy storage applications and delivers strategies for further developments in the performance of such type materials.

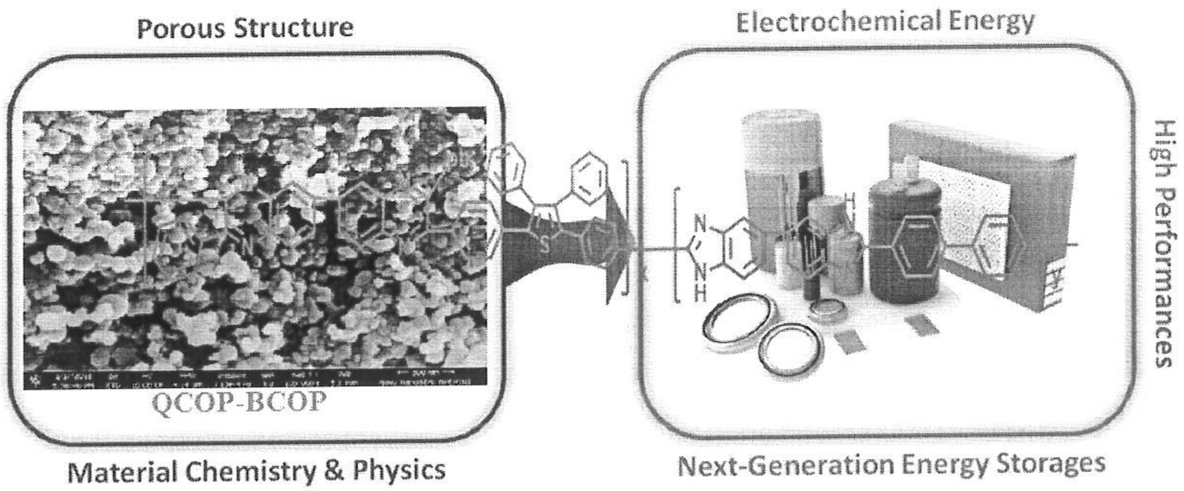

View Article Online
DOI: 10.1039/C9NJ02877C

Novel synthetic approach for designing metal free, redox active quinoxaline-benzimidazole based organic polymers with high energy storage capacity.

Pravin S. Salunkhe,[a,c] *Yuvraj S. Patil,*[a] *Indrajeet A. Dhole,*[b] *Basavraj S. Kalshetti,*[a] *Vikas B. Patil,*[b] *Shivshankar R. Mane,*[c] *and Anil A. Ghanwat*[a*]

a. Polymer Research Laboratory, School of Chemical Sciences, Solapur University, Solapur-413255, (MS), India.

b. Functional Materials Research Laboratory, School of Physical Sciences, Solapur University, Solapur-413255, (MS), India.

c. Polymer Science and Engineering Division, CSIR-National Chemical Laboratory, Pune

E-mail : **anil_ghanwat@yahoo.com**

ph.salunkhe@ncl.res.in

ABSTRACT:

A new organic framework materials polyphenylquinoxaline (QOP) and polyphenylquinoxaline-benzimidazole (QOP-BOP) has been designed through a high temperature (>100°C) polymerization reaction using different monomers 2, 5-bis-[(4- benzoylcarbonyl) phenyl] -3-4 diphenyl thiophene (BbcPDT), aromatic tetraamines and biphenyl dicarboxylic acid. QOP-BOP copolymer exhibited specific capacitance (SC) of 305 F/g current density at 2 A/g and 88 % retention of its initial specific capacitance after 1000 cycles resulted good cyclic stability.

This work establishes the first use of thiophene integrated with quinoxaline-benzimidazole units for energy storage applications and delivers strategies for further developments in the performance of such type conjugated materials. Cyclic voltammogram, charge-discharge and electrochemical impedance techniques are used to evaluate electrochemical parameters which advised its upcoming potential in energy storage devices.

KEYWORDS: Thermal stability, BbcPDT, Mesoporous polymer, Supercapacitor, Structure Property Relations.

INTRODUCTION:

Recently, a higher global environmental consciousness has sparked a widespread interest in the development of clean and efficient energy storage systems. As a result, organic polymer-based supercapacitors have been identified as environmentally beneficial energy storage systems due to their simple, clean, and efficient operation[1]. The carbon species, metals and conjugated polymer electrode materials are used for energy storage devices. In which carbon containing electrodes

View Article Online
DOI: 10.1039/C9NJ02877C

with decent conductivity and stability generally have better cycling stability and high-power density. Though, the energy density of these electrodes for capacitors are low because of limitation of mechanism of energy storage. The metal related electrodes may have brilliant energy storage response in supercapacitors because of their good activity but they still have difficulties like less conductivity and big cost.[2] To overcome the limits of carbon and metal electrodes synthesis of alternate electrodes such conjugated polymers (CPs) electrodes, like polypyrrole (Ppy), polyaniline (PANi)[3] and also prepared polymers have significantly attention towards energy storage/conversion, sensors as well as actuators and or many electrochromic devices. The C, H, N or S components are also show the high affordability in synthesized polymers. We need to return and look into organic redox-active materials for next-generation energy storage as active materials, because they have great advantages in terms of desirable molecular structure, superior chemical and physical properties, and excellent electrochemical storage performance compared with new inorganic electrode materials like Robust SnO^{2-x} Nanoparticle[4], black/red phosphorus hybrid[5], graphite/electrolyte interface[6] etc.[7] Therefore, organic redox-active materials can provide excellent solutions to further improve existing ESS technologies and a diverse basis from which to develop advanced ESSs. More precisely, redox-active polymers have been mainly utilized for ESS applications. rather than organic single molecules with same redox groups due to the well-known advantages of polymeric materials, such as good stability, excellent processability, and easy device fabrication.[8] Compared with electrochemical double-layer supercapacitors, the conjugated polymers-based devices showed improved specific capacitance and has quicker reaction kinetics[4] QOP and QOP-BOP are an important class of aromatic heterocyclic, it has the good thermal oxidative stability, batter thermoplastics properties and that have batter glass transition temperatures as well as tensile properties[9-12] similarly, these have good proton conductivity when appropriate doping.[13] Also, QOP are a historical and famous example of a phenyl-functionalized thermally stable polymer whose bulky phenyl group's leads to the increased solubility results higher processability as compared to the without phenyl functionalized polymer.[14-16] The π-conjugated organic polymers contain extended π-conjugation and have the inherent electrical conductivity because of extended π-conjugated skeleton andionic conductivity due to conduction of ions within the polymer backbones as promising candidate for the supercapacitor as well as sensor materials.[17-19] Furthermore, high processability and physicochemical properties inherent to polymers are ideal for investigation as supercapacitor materials.[20] Recently different such types of organic polymers are reported e.g. formation of C-N and C=N bonds as in the covalent organic frameworks via acid catalyzed condensation reactions,[21] benzimidazole linked polymers (BILPs)[22] and BILPs and synthesized quinoxaline

View Article Online
DOI: 10.1039/C9NJ02877C

linked polymers (PLPs) have been paid much attention from the science community due to the easy synthesis of the basic imidazole unit by the condensation of aldehyde and amine or quinoxaline unit by the diketone and tetraamines.

Recently, we reported azo based polyazomethines containing heterocyclic quinoxaline active redox unit into polymer backbone, it showed good electrochemical energy storage performance i, e. 252 F/ g.[23] Xu et al. reported a radical functionalized COF and is used as an electrode material. But the specific capacitance achieved is only 167 F/ g.[24] For MOF synthesized from carbon-based electrode material, the specific capacitance 251 F/g remain far low the expected level.[25] Jiang et al. and co-workers have also applied an azo fused π-conjugated microporous polymer as supercapacitor electrode material with storage capacity of 378 F/g documented.[26] These materials have good features for energy storage and conversion due to its mesopores nature for quick ion mobility which helps interfacial charge accumulation through the mesopores. The classical method for the synthesis of phenylated polyphenylquinoxaline was first reported by Hergenrother et al. in 1967 and it involves the cyclopolycondensation of aromatic bis(o-diamines) with aromatic tetra ketones in m-cresol.[27] Herein, we report a new high temperature synthetic strategy for designing a metal free, redox active quinoxaline and quinoxaline-benzimidazole based organic polymer via simple one-step polycondensation. The synthesized polymers have been evaluated as an electrode material for supercapacitor application and its interesting results highlights the potential of supercapacitor as a high-performance energy storage system for practical applications.

Experimental

Synthesis of 2, 5-bis-[(4- benzoylcarbonyl) phenyl] -3-4 diphenyl thiophene (BbcPDT):

BbcPDT monomer was prepared according to our previous reported literature[23]

Yield. 2.90 g (88.95 %), mp.140 °C. 1H-NMR: (400 MHz, $CDCl_3$ ppm) δ: 7.99 d (4H) J = 8.4 HZ, 7.85 d (4H) J = 8.4 Hz, 7.71-7.66 m (2H), 7.53 t (4H) J = 8.4 & 1.6 Hz, 7.38 d (4H) J = 8.8 Hz, 7.21-7.15 m (6H), 6.98 d (4H) J = 8.0 Hz.

Synthesis of polyphenylquinoxaline:

Polyphenylquinoxaline was synthesized by using the following general procedure (Scheme 1): DAB (0.214 g, 1 mmol) and BbcPDT (0.652 g, 1 mmol) were added in a 100 mL three neck round bottom flask in a nitrogen atmosphere. Polyphosphoric acid (20 g) was added to the flask and the mixture was stirred under a slow nitrogen purge. The polymerization temperature for the QOP homopolymer was 125 °C for 4.5 h. As the reaction continued, the viscosity of the solution increased, and the colour of the reaction mixture was changed from brown to deep red. The residual polymer solution in the flask was hydrolysed with distilled water. When hydrolysis of the solution is completed, then the reaction mixture was heated and neutralized with ammonium

View Article Online DOI: 10.1039/C9NJ02877C

hydroxide. The polymer was finally isolated and dried under vacuum to provide the polyphenylquinoxaline powder.

Synthesis of polyphenylquinoxaline-benzimidazole copolymer (QOP-BOP).

QOP-BOP copolymers were set across a wide range of QOP concentrations:

Diaminobenzidine (DAB) (2.52 g, 11.8 mmol), BPDA (0.977 g, 5.90 mmol), and BbcPDT (0.97 g, 5.90 mmol) were charged in a 100 mL three neck round bottom flask in a nitrogen atmosphere. Polyphosphoric acid (20 gm) was added in flask and the mixture was stirred by stirrer under a slow nitrogen purge. The reaction mixture temperature was increased stepwise to dissolve all the monomers in PPA, and then polymerize the QOP-BOP portions of the copolymer. For QOP-BOP, the polymerization temperature was held at 125 °C for 8 h, followed by an increase in temperature up to 195 °C for an additional 6 h. Note that the time at 195 °C varied based on the composition of the QOP-BOP copolymer, but the time necessary for low temperature QOP formation at 125 °C was constant across the QOP-BOP copolymer series. For all QOP-BOP copolymers it was needed to first obtain a highly viscous final polymer solution, followed by the addition of phosphoric acid to reduce solution viscosity in order to obtain a high inherent viscosity, polymer solution with good processability.

Result and discussion:

A new 2, 5-bis- [(4- benzoylcarbonyl) phenyl] -3-4 diphenyl thiophene (BbcPDT) was synthesized in 3 steps (Presented in scheme-1). QOP homopolymer and QOP-BOP copolymer were synthesized by polyconderisation of DAB with BbcPDT by high temperature synthetic strategy via PPA process (scheme 2 and 3). The composition of monomers yields, and viscosities of polymers are listed in Table 1. The structure of BcbPDT and BbcPDT was confirmed by spectroscopic analysis. Infrared spectrum of BcbPDT (Figure 1) showed a strong absorption band at 1684 cm^{-1} (>C = O) for aryl alkyl carbonyl structure and spectrum of BbcPDT showed a strong absorption bands at 1670 cm^{-1} for dicarbonyl (>C = O).

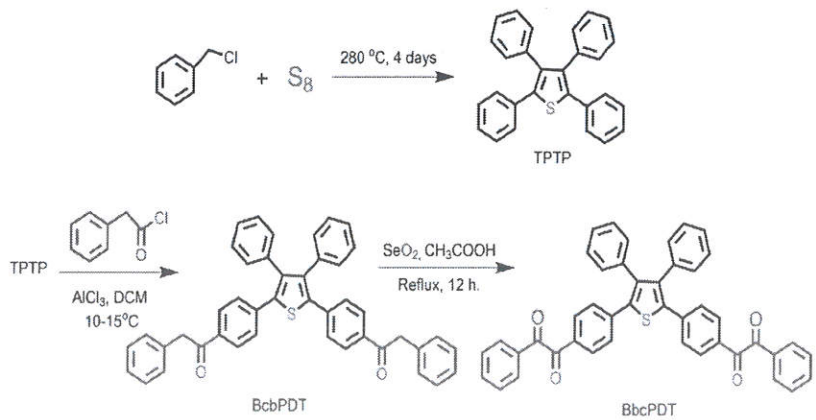

Scheme 1: Synthetic scheme for BbcPDT.

View Article Online
DOI: 10.1039/C9NJ02877C

Reagents and conditions:

a) Reflux, 240 °C, 3 days. b) $PhCH_2COCl$, $AlCl_3$, DCM 10-15 °C. c) SeO_2, Glacial Acetic Acid, Reflux 12 hrs.

^1H NMR of BcbPDT could not be taken due to insolubility of the compound BcbPDT even in chloroform, dimethyl sulfoxide or trifluoroacetic acid. The ^1H NMR spectrum of BbcPDT conform the structure assigned as evidenced by the chemical shift (all aromatic protons 8.07 to 7.1); number of NMR signals and expected multiplicity of the peaks with appropriate integration and no signals due to -CH, in the range of 1 to 6 ppm (Figure 2). ^{13}C NMR of BcbPDT (Figure 3) also consistence with the ^1H NMR spectroscopy. The two carbonyl carbon appeared at 193 and 194 ppm confirms formation of tetraketone monomer.

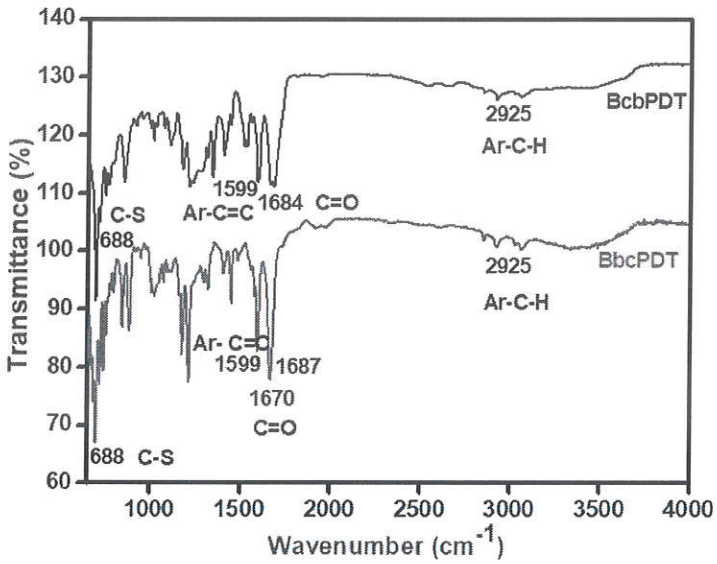

Figure 1. FTIR of BcbPDT and BbcPDT.

View Article Online
DOI: 10.1039/C9NJ02877C

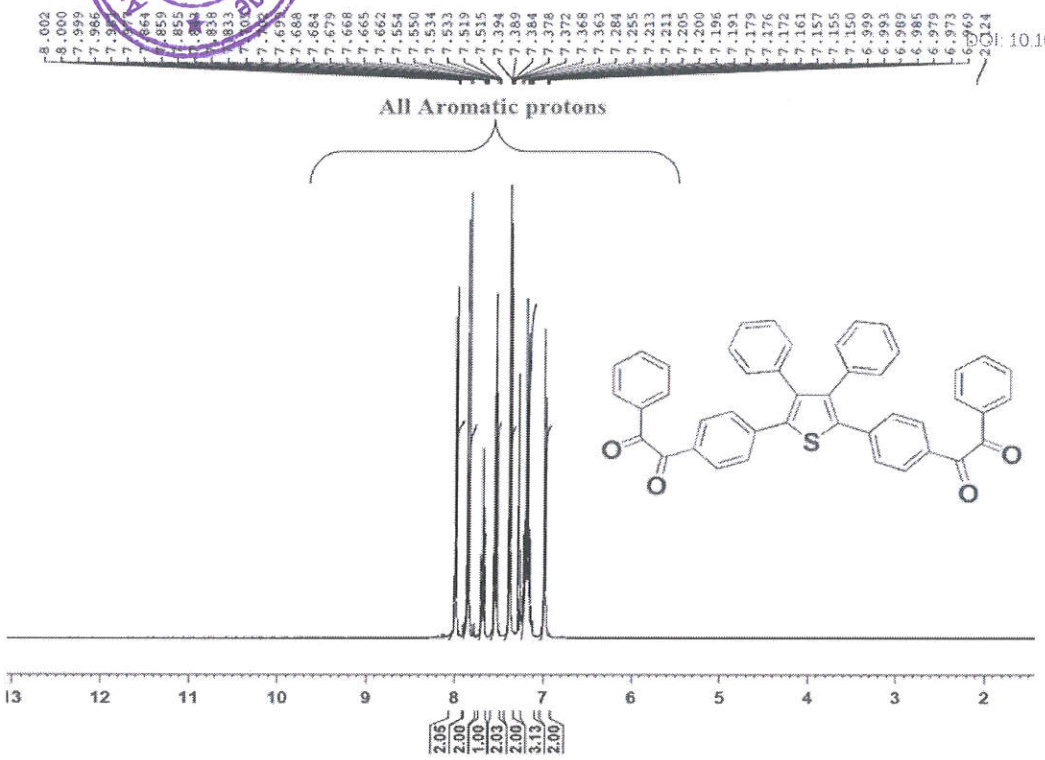

Figure 2: ^{1}H NMR of BbcPDT.

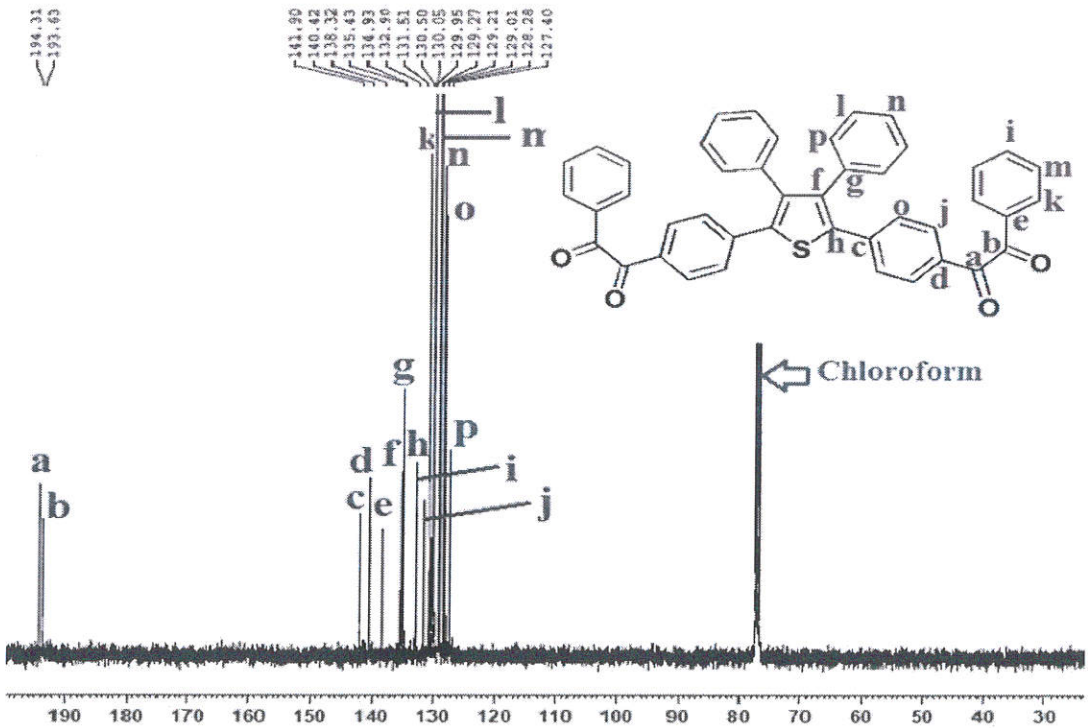

Figure 3: ^{13}C NMR of BbcPDT.

View Article Online
DOI: 10.1039/C9NJ02877C

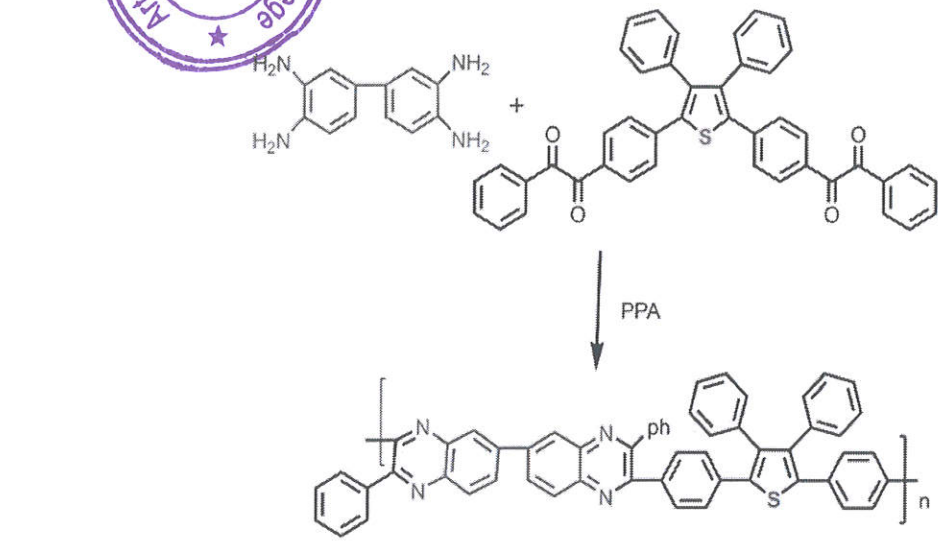

Scheme 2. Synthetic route for QOP homopolymer.

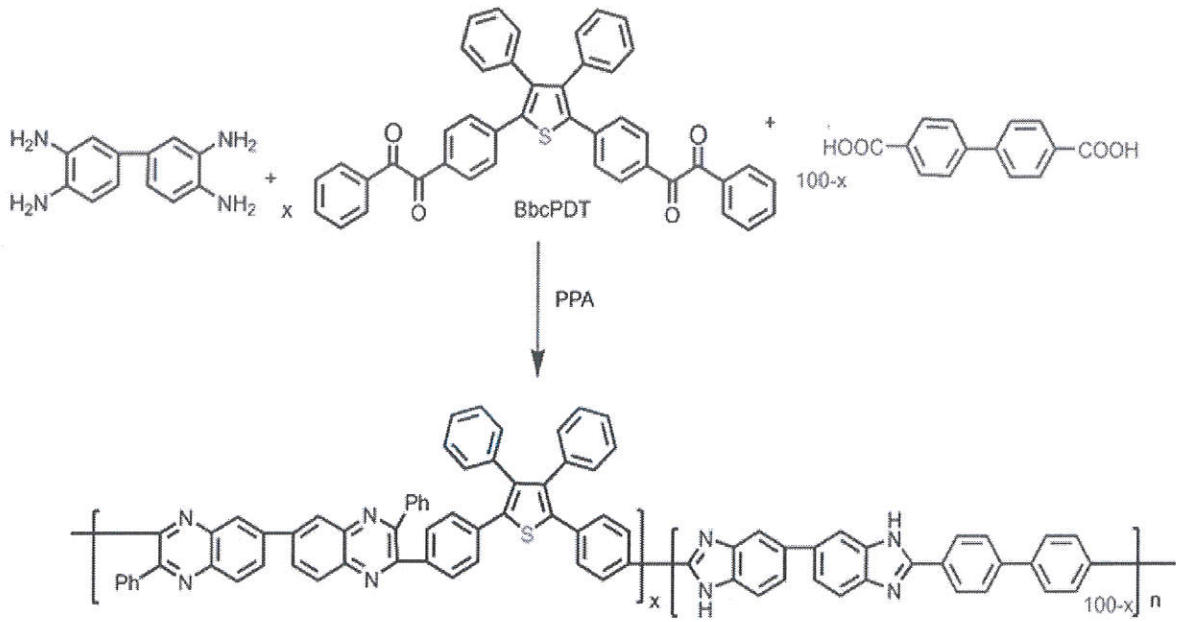

Scheme 3. Synthetic route for QOP-BOP copolymer.

View Article Online
DOI: 10.1039/C9NJ02877C

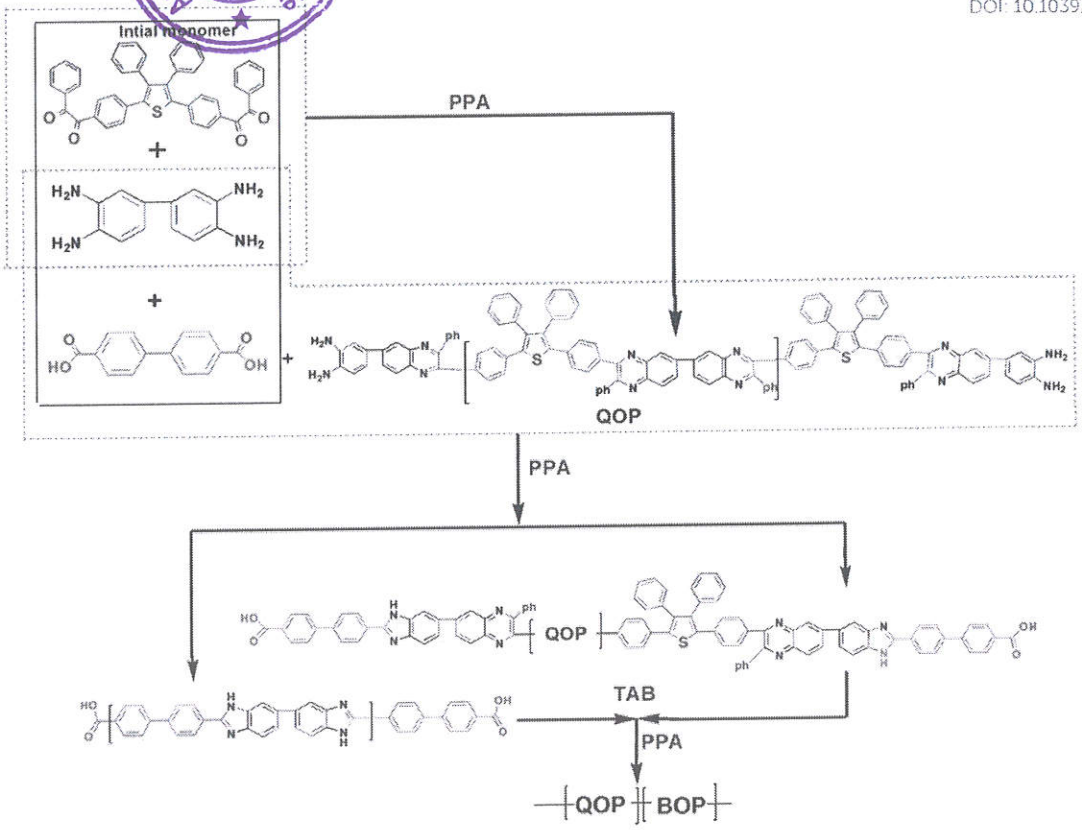

Figure 4: Mode of multi-block formation of QOP-BOP copolymer.

Figure 4 showed multi-block formation of copolymer containing quinoxaline and benzimidazole unit. The formation of polymer was confirmed by FTIR and NMR spectroscopy. Figure 5 showed the FTIR spectra of polymers. FTIR spectrum of QOP showed absence of absorption band at 1670 cm^{-1} indicating ketonic functionality of BbcPDT reacted completely to form QOP. Similarly, absorption at 3400-3000 cm^{-1} due to NH (stretch) was absent. Infrared spectrum of QOP and QOP-BOP showed a strong absorption band at 1598 cm^{-1} and 1605 cm^{-1} for imine nitrogen(s) (C=N).

View Article Online
DOI: 10.1039/C9NJ02877C

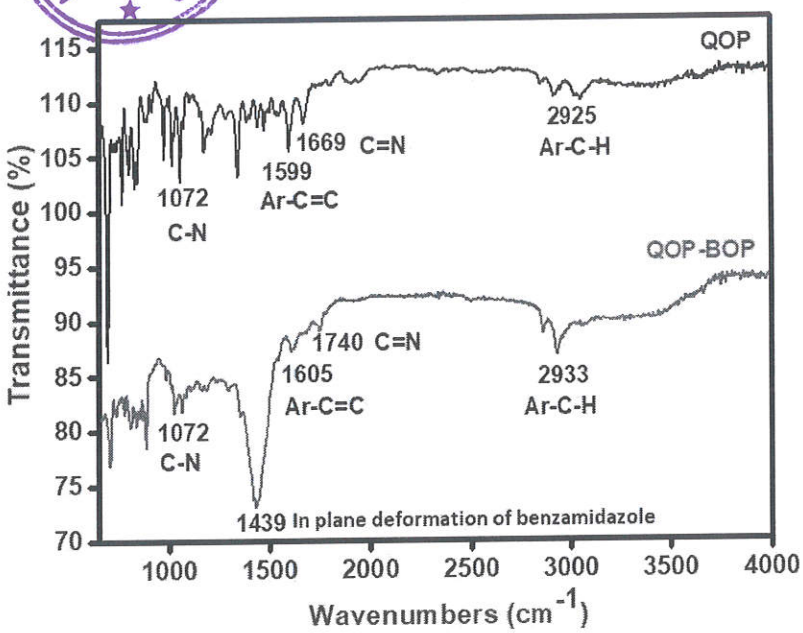

Figure 5: FTIR spectra of QOP and QOP-BOP.

Figure S-1 showed the ^1H NMR spectra of QOP (because of poor solubility of QOP in DMSO, so $CDCl_3$ were used). All aromatic protons were well assigned to the supposed chemical structure. The integration ratio of the peaks corresponded to the polymer composition expected from the feed monomer. Aromatic protons were strongly shielded, and their signals appeared at low frequency (7.0-7.9 ppm) area, while the protons located at ortho-positions of –C=N– were deshielded due to their strongly electron-withdrawing effects, and their signals appeared at high frequency area (7.9-8.6 ppm). No characteristic chemical shift of $–NH_2$ (around 5 ppm) was observed, which also indicated that a fully cyclization of quinoxaline has been attained through the polymerization progress. NMR of QOP-BOP could not be taken due to insolubility even in chloroform, dimethyl sulfoxide or trifluoroacetic acid.

Thermal properties and crystallinity:

Thermal properties of synthesized polymers were evaluated by thermogravimetry and results are given in figure 6 and table-1. The polymers showed the initial decomposition temperature between 205 to 273 °C and T_{10} in the range of 433 to 779 °C whereas the residual weight at 900 °C was in the range of 57 to 68 % it indicates that the polymers are highly thermally stable.

View Article Online
DOI: 10.1039/C9NJ02877C

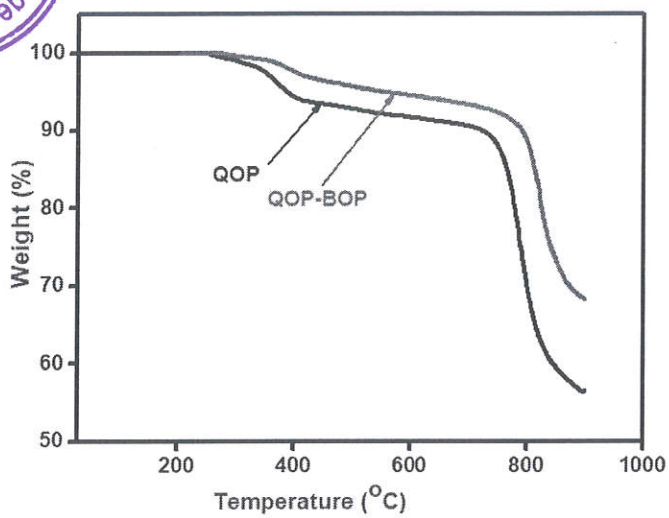

Figure 6: TGA curves of QOP and QOP-BOP.

The glass transition temperatures (Tg) of the polymers evaluated from the DSC curves (figure-7). They were in the range of 256-291 °C. QOP showed no evidence of crystalline peaks, which proves an amorphous morphology result slightly, lowers the glass transition temperature. This decrease in Tg is due to the increase in the flexibility of the polymer backbone due to the pendent phenyl groups present in monomer segment.

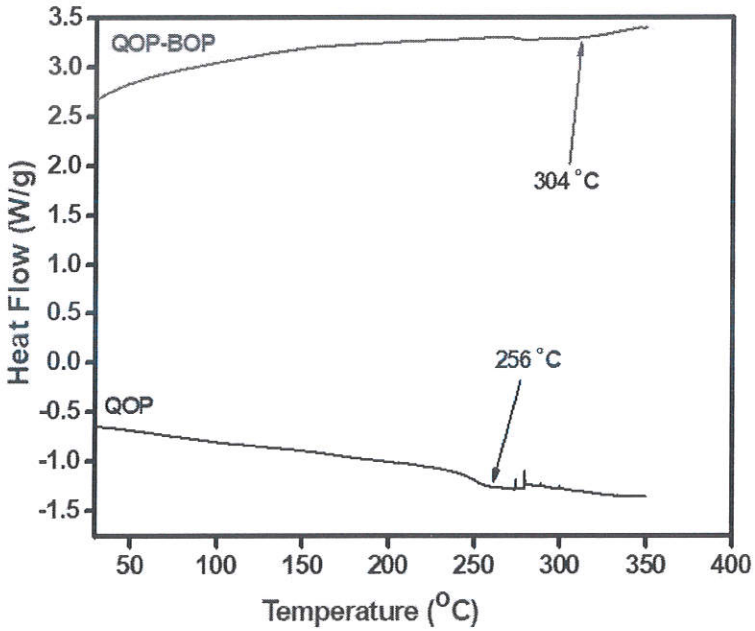

Figure 7: DSC curves of QOP and QOP-BOP.

As shown in figure 8 the crystallinity of synthesized polymer films was analysed by wide angle X-ray diffraction. The WAXD patterns of QOP showed broad peak, which indicated that it is more amorphous pattern. The QOP-BOP also showed broad peak with some crystalline peaks was in polymer backbone which indicated that it was less amorphous

View Article Online DOI: 10.1039/C9NJ02877C

pattern. Some crystalline peaks were observed in QOP-BOP may be due to rigid benzimidazole unit in polymer backbone. The more amorphous nature of QOP can be mainly explained by the introduction of bulky pendent groups and then greatly decrease the crystallinity of polymers.

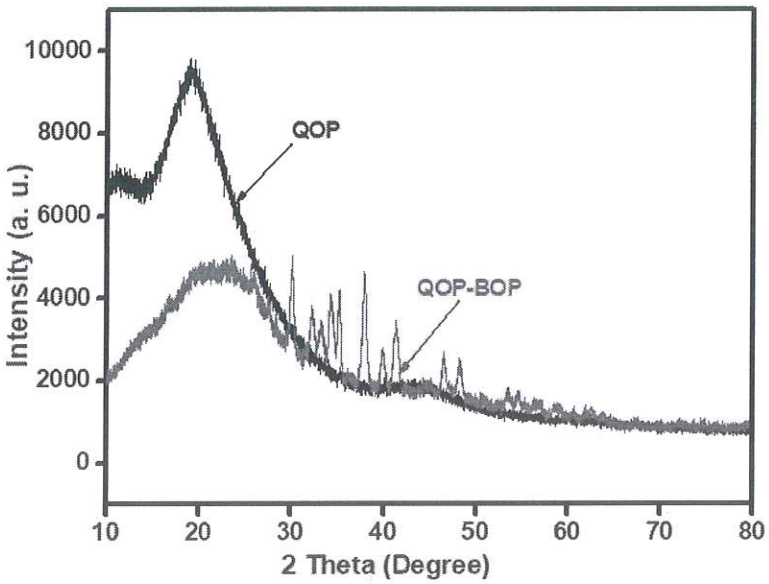

Figure 8: WAXD of QOP and QOP-BOP.

Polymer solubility yield and viscosity.

QOP homopolymer was soluble in chloroform, tetrachloroethane, tetrahydrofuran and m-cresol etc. QOP-BOP copolymer was soluble in tetrahydrofuran and m-cresol etc. However, they are partly soluble in aprotic polar solvents such as dimethylacetamide (DMAc), dimethylformamide (DMF) and N-methylpyrrolidone (NMP) and partly soluble in chlorinated solvents. These polymers were insoluble dimethyl sulfoxide (DMSO). A 3 % solution was taken as criterion for solubility. On qualitative comparison, it was observed that the polymers containing higher % of BbcPDT i.e. QOP was more easily soluble than QOP-BOP.

Table 1: Yield, viscosity and thermal properties of QOP and QOP-BOP from TAB.

Polymer Code	Yield (%)	Viscosity (dL/g)	Thermal Properties		Residual Weight at 900 °C (%)	Glass Transition Temperature (Tg)
			T_i (°C)	T_{10} (°C)		
QOP	98	0.63	245	663	57	256
QOP-BOP	99	0.82	273	779	68	304

View Article Online
DOI: 10.1039/C9NJ02877C

Morphology and surface wettability study:

FE-SEM image of QOP figure 9 (a) shows the nanoparticles like morphology which have some particles aggregations are also occurred. The figure 9 (b) obviously shows that the nanoparticles which are homogeneous and well defined with particles have a narrow size distribution with an average size of 100-170 nm.

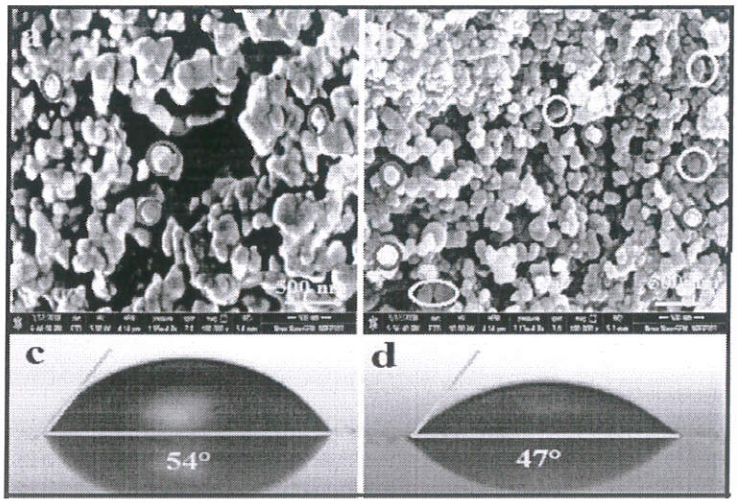

Figure 9: FE-SEM images QOP (a) and QOP-BOP (b). Water contact angle measurements of QOP (c) and QOP-BOP (d).

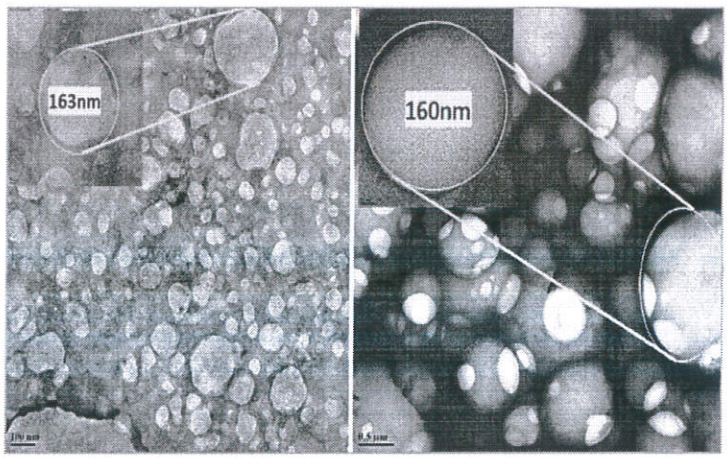

Figure 10: TEM images QOP (a) and QOP-BOP (b).

TEM images of QOP and QOP-BOP (figure 10) consistence with the FE-SEM results. Energy dispersive X-ray spectroscopy (supporting information figure S-2, section S-3) shows the peaks around 0.1 and 2.3 KeV are related to the energies of S, along with the peak of nitrogen and carbon at 0.4 and 0.3 KeV respectively. Therefore, the EDX confirmed the presence of sulphur, nitrogen and carbon in QOP-BOP. The atomic percentages obtained from EDX quantification were 85.93% of C, 12.88% of N and 1.19% of S. To study the contact at the electrode/electrolyte interface, a wettability test was carried out. The average contact angle was acquired by measuring for at least five separate drops on polymer film

View Article Online
DOI: 10.1039/C9NJ02877C

surface by delivering deionised water. Measurement of surface water contact angle is inversely proportional to the wettability and can be determined by Young's relation. Figure 9 (c and d) shows the digital photograph of water contact angle measurement on synthesized polymer electrode surfaces. Interestingly QOP and QOP-BOP electrode surfaces has exhibited hydrophilic behaviour with 54° and 47° water contact angle values respectively. i.e. < 90°. Generally, low water contact angle (hydrophilic behaviour) increases the electrochemical performance, where interfacial contact at electrolyte-electrode is considerably high.[28, 29] The surface of QOP and QOP-BOP thin films is hydrophilic which is useful for forming intimate contact between aqueous electrolyte and thin films in supercapacitors. Due to the mesoporous nature of synthesized polymers, water can easily intercalate inside the pores. Thus, positive ions in aqueous electrolyte can easily intercalate or de-intercalate, i.e. ionic conductivity increases and hence the supercapacitance increases.

Surface area and pore size distribution:

The samples were characterized by nitrogen adsorption and desorption isotherms at 77 K as shown in figure 11 (a and b). This isotherm shows nitrogen uptake at 1 bar pressure suggestive of porous nature of the synthesized polymers. In terms of shape, the isotherms of the QOP and QOP-BOP structures show hysteresis loops that specify the presence of mesopores with size ranging from 2 to 50 nm.[30] QOP and QOP-BOP samples show BET surface areas of 45.851 m^2/g and 11.056 m^2/g respectively. These data indicate that the QOP have a larger surface area than the QOP-BOP. The measured BET surface area of QOP-BOP (11.056 m^2/g) was lower than QOP. It is noticing that the polymer reported here is copolymer containing only a small amount of comonomer. Speciously, at such low comonomer content, its impact on surface area is limited.[31] Many polymers reported in the literature are homopolymers containing large amounts of conformationally rigid monomers whose effect on surface area is considerable. It is supposed that in such isotherm's ascorbate-adsorbent interactions play an important role. The adsorption isotherms show a slow increase in middle level relative pressures and a steeper increase at higher pressures. Such behaviour has been reported previous as characteristic of mesoporous.[32] The BJH pore size distributions plots (figure 11 c and d) of QOP and QOP-BOP showed a narrow distribution which designated that the pores size was homogeneous. The average pore sizes calculated using the BJH equation from the adsorption branch of the isotherms of QOP and QOP-BOP was found to be 23.4 and 21.2 Å respectively. Pore size distribution was estimated by fitting the uptake branches of the nitrogen isotherm with nonlocal density functional theory and half pore width of QOP and QOP-BOP found to be 10 Å and 13 Å respectively as well as pore

volume is 0.100 and 0.022 cc/g respectively. NLDFT data presented in supporting information section S-5 and figure S-6.

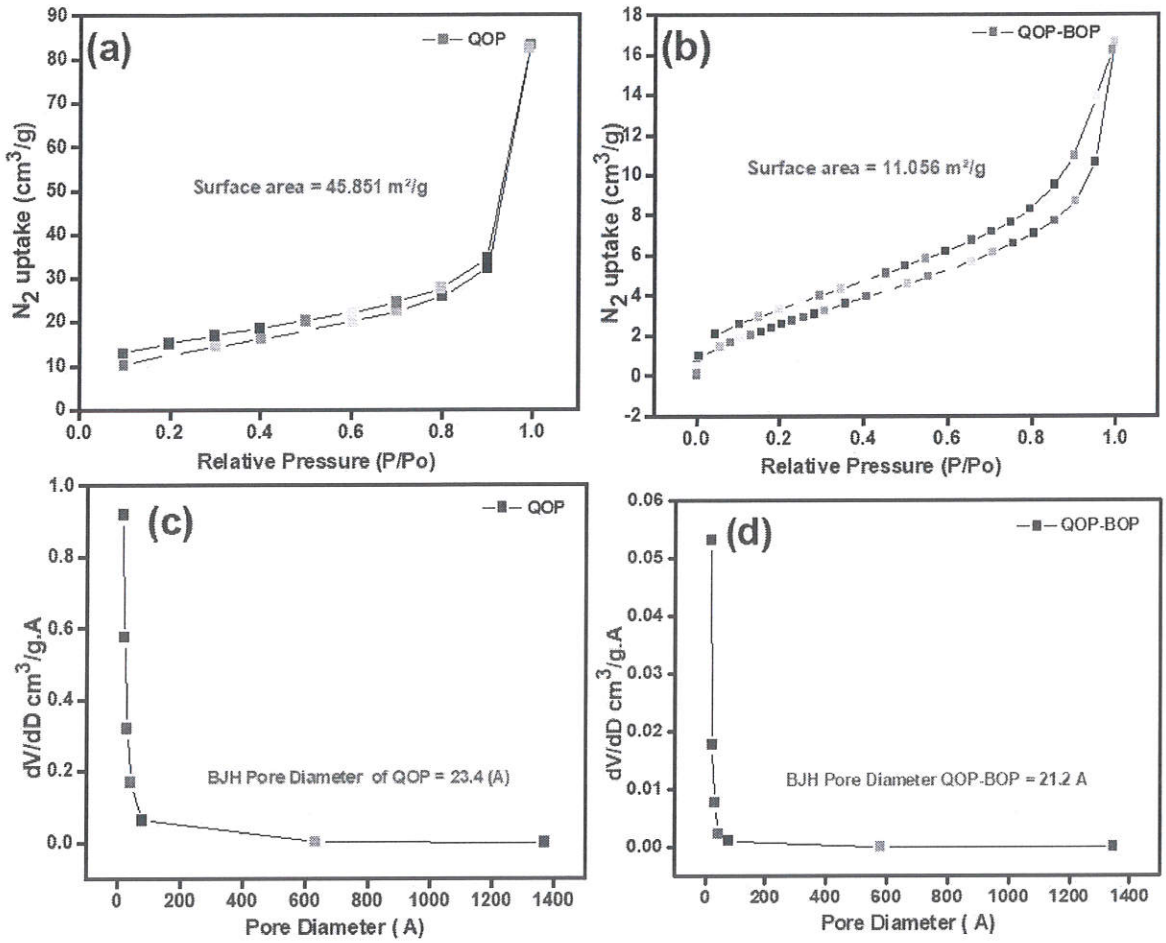

Figure 11: N_2 Adsorption-desorption isotherm of QOP (a) and QOP-BOP (b). BJH pore size distribution plots of QOP (c) and QOP-BOP (d).

Electrochemical analysis:

The electrochemical charge storage activity of the prepared QOP and QOP-BOP electrode materials was analysed by cyclic voltammetry (CV) galvanostatic charge discharge (GCD) and electrochemical impedance spectroscopy (EIS) in 1 M Na_2SO_4 electrolyte. For the three-electrode systems, saturated calomel electrode (SCE) served as the reference electrode, platinum acted as the counter electrode and the prepared electrode (1 cm^2) was used as working electrode. The working electrode was fabricated by dissolving active material in chloroform, then coated on the stainless-steel substrate (1 cm^2) and heated at 50 °C in vacuum oven for 10 hrs. The mechanism of the polymer QOP-BOP is presented in Figure 12. Firstly, the nitrogen of benzimidazole as well as quinoxaline in QOP-BOP oxidized at low applied potential and loses one electron to form the benzimidazole and quinoxaline radical

View Article Online
DOI: 10.1039/C9NJ02877C

cation, which is equivalent to the resonance form II. In II, the electron pair and the single electron are both in sp^3 hybrid orbitals. Owing to the distinct coplanar structure between quinoxaline, benzimidazole and thiophene, there are three resonance forms (II, II#, and II*) of this radical, representing the delocalization of the single electron over the quinoxaline, benzimidazole and thiophene units, the most stable form of which should be II* where the single electron is on the thiophene unit. The mechanism involved in QOP is same as QOP-BOP.

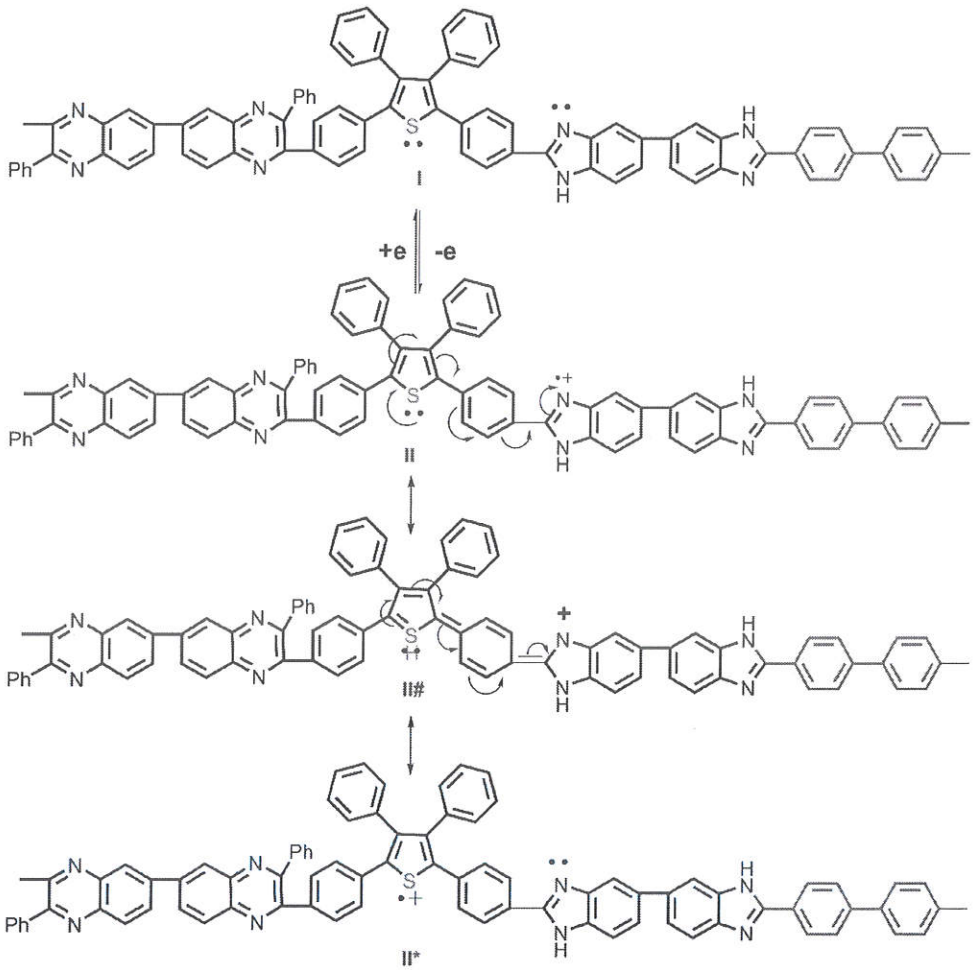

Figure 12. Electrochemical mechanism for oxidation of QOP-BOP.

The CV recorded with prepared QOP electrode over different scan rates, it shows redox peaks at ~ -0.5 V during forward (anodic) and backward (cathodic) sweep it suggested that its pseudo capacitive nature[33] while for QOP-BOP material, when a potential is applied to a pseudocapacitor cell oxidation and reduction takes place on the polymer electrode material, which involves the passage of charge across the double layer, resulting in faradic current passing through the supercapacitor cell. The faradic process involved in pseudocapacitor allows them to improve specific capacitance compared to electrical double layer capacitors. Pseudocapacitor store charge via faradic process which involves the transfer of charge

between electrode and electrolyte.[34] Further the lengthening of peaks indicates the insertion of ions onto the electrode materials.[35] The specific capacitance of the electrode material is estimated from following equation,

$$Csp = \int (IdV)/vmV \quad (1)$$

Where I is response current, V is potential window, v is potential scan rate, and m is mass of the active materials respectively. The electrochemical properties of polymer films were investigated in aqueous media viz. 1M Na_2SO_4 as electrolyte at different scan rates because the resistance of the supercapacitor material is independent on the resistivity of the electrolyte and the size of ions from the electrolyte. The organic electrolytes have a greater resistance, but the adjunct power reduction is usually offset by the increase in higher cell voltage. This is usually not a problem for an aqueous electrolyte and aqueous electrolytes are cheaper as well as it purifies easily.[36] Moreover, the concentration of electrolytes increases, specific capacitance also increases due to the take off the material from substrate, so greater than 1 M concentration was avoided.[37] Usually, the CV curve of polymers shows a typical rectangular shape without redox peaks, and the energy is stored by electrical double-layer (EDL) between polymer electrode materials and electrolytes (non-faradic mechanism)[38, 39] Typical CV curves of the synthesized polymers in 1M Na_2SO_4 measured at various scan rates are given in figure 13 (a and b).

View Article Online
DOI: 10.1039/C9NJ02877C

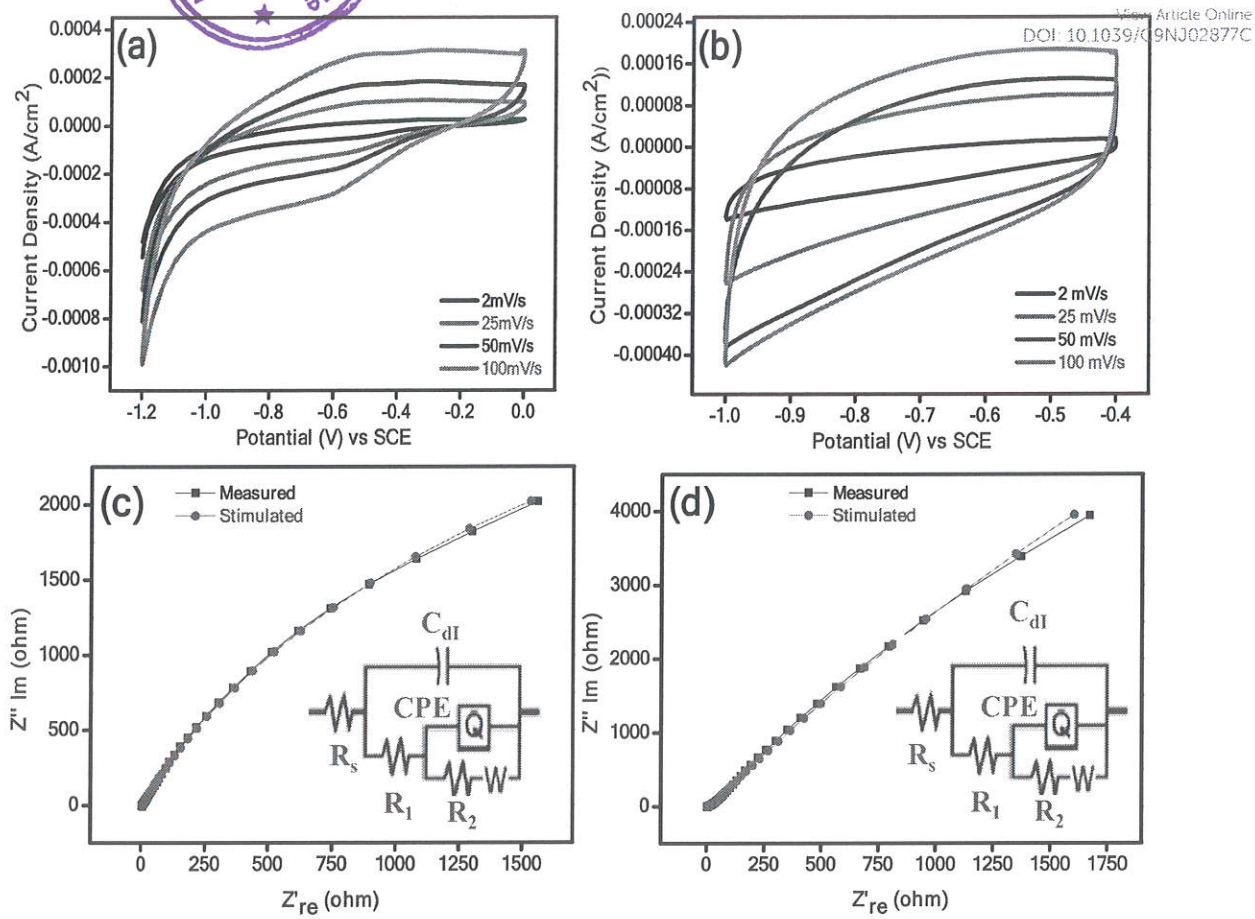

Figure 13: comparison of CV curves of QOP(a) and QOP-BOP (b) thin film electrode at different scan rates of 2, 25, 50 and 100 mV/s in 1 M Na_2SO_4 electrolyte. Electrochemical impedance spectra of QOP(c) and QOP-BOP (d).

The CV curves of synthesized QOP and QOP-BOP shows redox peaks therefore, the capacitance of synthesized polymer materials is mainly based on redox reactions (faradic mechanism).[40] The shape of the CVs for these synthesized polymers remains unchanged from 2 to 100 mV/s indicating good rate properties. Another proof, for good rate ability of these materials is the current increases with the scan rates, as can be seen in figure 13. It showed that the specific capacitance changes with the change in scan rate, so that higher specific capacitance was observed at low scan rate. (The scan rate vs sp. capacitance figure given in supporting information section S-4). As the scan rate, has increased, the specific capacitance has decreased, which may be explained by the increase of ions concentration at the electrode/electrolyte interface while the diffusion rate of electrolyte from electrolyte/electrode interface remain limited to assure electrochemical reactions.[41] The QOP and QOP-BOP polymers documented maximum specific capacitance of 36 and 59 F/g is at 2 mV/s scan rate.

View Article Online DOI: 10.1039/C9NJ02877C

In case of conjugated polymer films, due to the electrochemically active nature of the polymer itself, a highly adaptable technique such as the electrochemical impedance spectroscopy (EIS) is ideal to accommodate the complex processes involved. Traditionally, EIS is applied to study the AC polarography and in determining double layer capacitance at the electrodes.[42] Electro-active polymers have been widely studied in last two decades because of their potential applications such as in electrocatalysis, energy storage, and sensors. In the current article, the electrochemical features of prepared QOP and QOP-BOP electrode surfaces were subjected to EIS analysis. The Nyquist plots of these polymer films deposited on stainless steel plate are shown in figure 13 (c and d). An equivalent circuit has been used to collect valuable information about different electrochemical parameters defining the process.[43] The equivalent circuit and parameter values by fitting the impedance data of QOP and QOP-BOP films to equivalent circuit shown in figure 13 and table S-1 (supporting information section S-3). The model circuit comprised of eight elements, the solution resistance (R_s) was in series with the electrical double layer capacitance (C_{dl}) at the electrode and electrolyte. C_{dl} was in parallel with R_1 and (R_2, W, and Q or CPE) is used to evaluate the different resistive and capacitive characteristics of QOP and QOP-BOP electrode. The Warburg impedance was associated with the semi-infinite diffusion of ions in the QOP and QOP-BOP electrode[44] suggested its good electrocapacitive activity. EIS measurement of QOP and QOP-BOP electrode measured within the frequency range of 1 MHz to 0.1 Hz in 1 M Na_2SO_4 electrolyte.

The charge-discharge measurements of the synthesized electrodes were carried out by using chronopotentiometry from -1.00 to 0.0 and -1.0 to -0.4 V respectively at different current densities as shown in figure 14 (a, b). The shape of the measured charge and discharge curves is not an ideal straight line, indicating that the observed behaviour is a result of the faradic type of redox reaction[45] The charging process of polymer electrode occurs above -1.0 V in the Na_2SO_4 electrolyte because of the oxidation and in the discharging process, no potential drop is observed indicates a good interfacial contact between the active material and the substrate during the charge-discharge process[46] All the GCD profile (figure 12 a, and b) showed near triangular characteristics resulting ideal charge storage behaviour. It is quite important to note that the discharge consists of two characteristics region having different discharge rate. First region is the rapid decay up to -0.4 and -0.5 V and then slow decay over rest potential window. The rapid decay is responsible for the EDLC formation and slow decay contributed from charge stored via redox reaction at electrode surface i. e,

View Article Online DOI: 10.1039/C9NJ02877C

pseudocapacitance.[22] The specific capacitance of prepared QOP and QOP-BOP polymers over different current density is estimated from following equation,

$$Csp = (I.\ \Delta t) / (\Delta v.\ M) \quad (2)$$

Where, *'I'* represents the applied current, *Δv* stands for potential range (*V*) and Δ*t* denotes the discharge time (s) and 'm' signifies mass of active material.

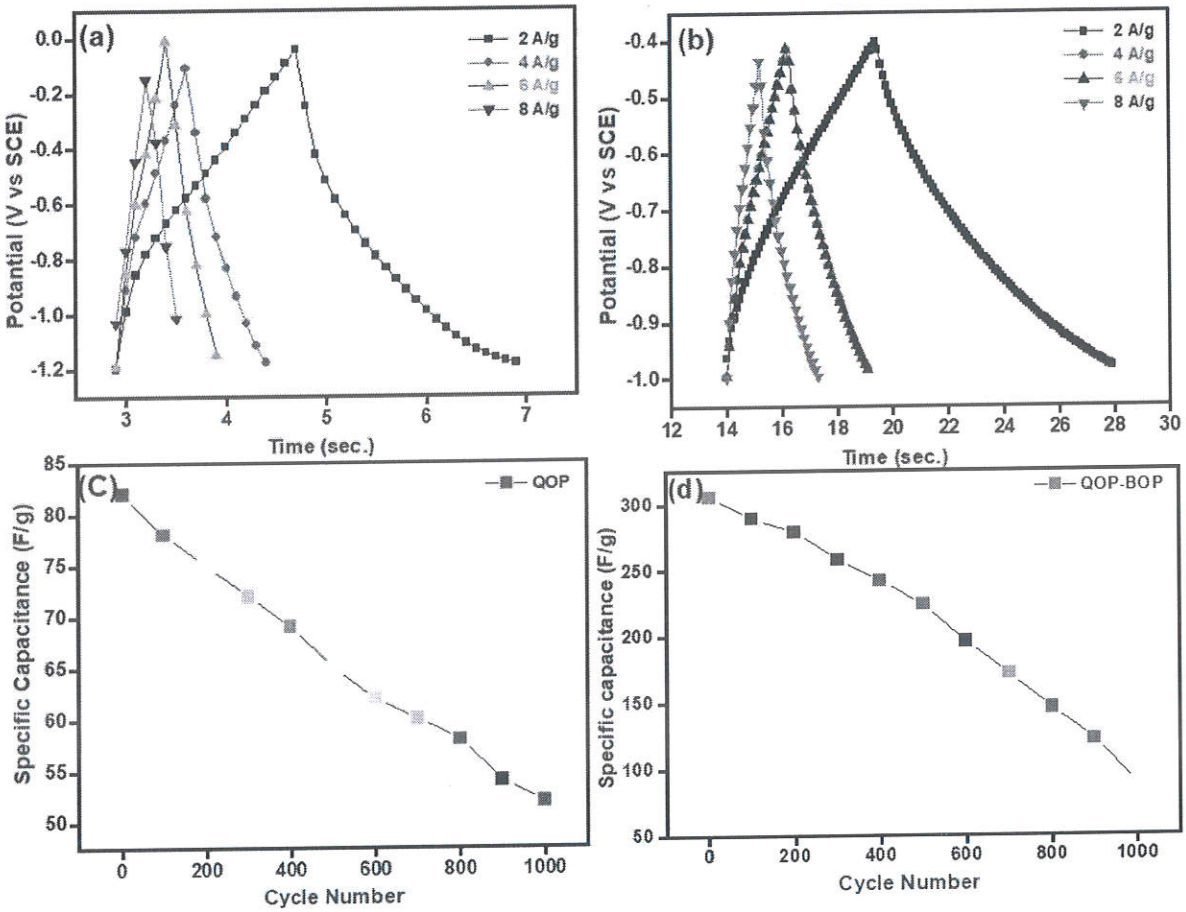

Figure 14: Galvanostatic charge–discharge curves of QOP (a) and QOP-BOP (b) electrodes. Cycling performance of QOP (c) and QOP-BOP (d) electrodes (capacitance as a function of cycle number).

A maximum specific capacitance of QOP-BOP is 305 F/g documented at 2 A/g current density. The high specific capacitance attained with the present QOP-BOP electrode is credited to the presence of redox active imidazolium and quinoxaline moiety. The obtained energy storage performance of the synthesized polymer material found to be outstanding than β-ketoenamine-linked covalent organic framework[47a] and conjugated microporous polymer[47b] (48 at 0.1 A/g and 252 at 1A/g) respectively and radical functionalized COF (167 F/g at 0.1 A/g).[48] Moreover, the specific capacitance of QOP-BOP is comparable with the reduced graphene oxide hydrogels (252.6 F/g at 1 A/g),[49] N-rich hollow carbon sphere (230

View Article Online DOI: 10.1039/C9NJ02877C

F/g at 1A/g),[50] the hierarchically porous carbon-AS-ZC-800 (251 F/g at 0.25 A/g),[51] interconnected microporous carbon (258 F/g at 0.5 A/g),[52] and nitrogen enriched porous carbon sphere (388 F/g at 1 A/g).[53] Additionally, the specific capacitance of QOP-BOP electrode material is analogous to metal oxide and oxide base nano composite materials, like $HTiO_2$ nanocrystal/N-doped graphene (385.2 at 1A/g),[54] PANI-doped graphene composite (480 F/g at 0.1 A/g)[55] and MnO2/CNT (201 at 1 A/g).[56] Thus, the present metal free QOP-BOP can be used as a potential electrode material for electrochemical energy storage and the structural restriction of covalent organic framework limits charge storage, which is completely absent on QOP-BOP electrode material. The cyclic stability of prepared QOP and QOP-BOP electrodes has been tested for 1000 cycles at 2 A/g current density and shown in figure 14 (c and d). The present QOP and QOP-BOP electrodes retain 52 and 88 % of its initial specific capacitance after 1000 cycles resulting excellent electrode material for supercapacitor application.

CONCLUSION:

We have designed new high temperature (>100 °C) polymerization method for the preparation of non-cross linked QOP homopolymer and multi-block QOP-BOP copolymer via PPA process. The resulting polymers were highly thermally stable and soluble in some organic solvents. Presence of characteristics bands and expected elemental peaks of monomer and polymer was confirmed from FTIR and NMR spectroscopy. The XRD patterns showed that the QOP and QOP-BOP have amorphous nature. Thermogravimetric analysis of polymers showed 10 % weight loss in the range of 433 to 779 °C indicating good thermal stability. The SEM picture of the QOP and QOP-BOP powder shows that the spherical nanoparticles. They are homogeneous with average size of about 100-170nm. The 51 and 47° water contact angle values of QOP and QOP-BOP was evidenced from the surface wettability measurement test, which favours for an excess infiltration of electrolyte ions for more redox reactions through wide range of area coverage. QOP-BOP electrodes have demonstrated a maximum specific capacitance of 305 F/g at 2 A/g in 1 M Na_2SO_4 electrolyte. The overall improved electrochemical performance of the copolymer QOP-BOP electrode prepared via high temperature PPA method makes it a promising material for potential applications in high performance supercapacitors because of its low cost, simple preparation and environmental friendliness.

ACKNOWLEDGEMENT

The author AAG thanks to University Grant Commission, New Delhi for financial assistance in the form of major research project. (Scheme No.: -UGC-MAJOR-MRP-CHEM-2013-

39804). Author would like to thank Dr. Prakash P. Wadgaonkar for BET surface area measurement.

View Article Online
DOI: 10.1039/C9NJ02877C

CONFLICTS OF INTEREST

There are no conflicts to declare.

REFERENCES:

1. A. Michel Petit, *J. Electrochem. Soc.,* 1993, **140**, 2498-2500.
2. W. Huanhuan, L. Jianyi, S. Ze Xiang, *Journal of Science: Advanced Materials and Devices.* 2016, **1**, 225-255.
3. S. Bhadra, D. Khastgir, N. Singha, Lee, *J. Prog. Polym. Sci.* 2009, **34**, 783-810.
4. Ma, Dingtao, Li. Yongliang, Mi. Hongwei, Luo. Shan, Zhang. Peixin, Zhiqun. Lin, Li. Jianqing, Zhang. Han, Angew. Chem. Int. Ed. 2018, **57**, 8901 –8905.
5. Chen, Xinhang, Xu. Guanghua, Ren. Xiaohui, Li. Zhongjun, Qi. Xiang, Huang. Kai, Zhang. Han, Huang. Zongyu, Zhong. Jianxin, J. Mater. Chem. A, 2017, **5**, 6581.
6. Wang. Renheng, Li. Xinhai, Wang. Zhixing, Zhang. Han, Nano Energy 2017, **34**, 131-140.
7. T.B. Schon, B.T. McAllister, P. F. Li, D.S. Seferos, Chem. Soc. Rev. 2016, **45**, 6345-6404.
8. N. Casado, G. Herna ndez, H. Sardon, D. Mecerreyes, Progr. Polym. Sci. 2016, **52**, 107–135.
9. G. Snook, P. Kao, A. Best, *J. Power Sources,* 2011, **196**, 1-12.
10. P. Hergenrother, *Appl. Polym. Symp.* 1973, **22**, 55-76.
11. Y. Patil, J. Mahindrakar, P. Salunkhe, V. Ubale, A. Ghanwat, *J. Macromol. Sci, Part A.* 2018, **55**, 572-581.
12. D. Klein, D. Modarelli, F. Harris, Macromolecules, 2001, 34, 2427–2437.
13. R. Kopitzke, C. Linkous, H. Anderson, N. Randolph L. Gordon, *J. Electrochem. Soc.* 2000, 147, 1677.
14. P. Salunkhe, S. Ankushrao, Y. Patil, J. Mahindrakar, V. Kadam, V. Ubale, A. Ghanwat, *J. Macromol. Sci, Part A.* 2018, **55**, 377-383.
15. Y. Patil, P. Salunkhe, J. Mahindrakar, S. Ankushrao, V. Kadam, V. Ubale, A. Ghanwat, *J. Therm. Anal. Calorim.* 2018, DOI: 10.1007/s10973-018-7567-2
16. P. H. Salunkhe, Y.S. Patil, V. N. Kadam, S.S Ankushrao, V. P. Ubale, A. A. Ghanwat. Polym. plastic tech. and materials. 2019, https://doi.org/10.1080/25740881.2019.1625385

17. S. Kandambeth, A. Mallick, B. Lukose, M. V. Mane, T. Heine, Banerjee. *J. Am. Chem. Soc.* 2012, **134**, 19524-19527.

18. Y. S. Patil, P. H. Salunkhe, Y. H. Navale, V. B. Patil, V. P. Ubale, A. A. Ghanwat, Polym. Bulletin. https://doi.org/10.1007/s00289-019-02856-2

19. Y. S Patil, P. H. Salunkhe, Y. H. Navale, V. P. Ubale, V. B. Patil, N. N. Maldar, A. A. Ghanwat, AIP Conference Proceedings, 2018,**1989**, 020034.

20. Deepak M. Maher, Samadhan S. Nagane, Uday. A. Jadhav, Pravin. H. Salunkhe, Bhausaheb. V. Tawade, Prakash. P. Wadgaonkar, J. Polym. Sci. Part A. 2019, **57,** 1516-1526.

21. S. Altarawneh, T. Islamoglu, Sekizkardes, A. K., ElKaderi, H. M., *Environ. Sci. Technol.,* 2015, **49**, 4715-4723.

22. C. Bidhan, Santimoy, Khilari., Lanka, Satyanarayana., Debabrata, Pradhan., Asim, Bhaumik. *Chem. Commun.,* 2016, **52**, 7592-7595.

23. P. Salunkhe, Y. Patil, Y. Navale, I. Dhole, V. Ubale, N. Maldar, A. Ghanwat, *Journal of Polymer Research*, 2018, **25**, 147.

24. F. Xu, H. Xu, X. Chen, D. Wu, Y. Wu, H. Liu, C. Gu, R. Fu, D. Jiang, *Angew. Chem. Int. Ed.,* 2015, **54**, 6814-6818.

25. R. Salunkhe, Y. Kamachi, N. L. Torad, S. M. Hwang, Z. Sun, S. X. Dou, J. H. Kim, Y. Yamauchi, *J. Mater. Chem. A,* 2014, **2**, 19848-19854.

26. Y. Kou, Y. Xu, Z. Guo, D. Jiang, *Angew. Chem. Int. Ed.,* 2011, **50**, 8753-8757.

27. P. Hergenrother, H. Levine, *J. Polym. Sci. Part A.* 1967, **5**, 1453.

28. Y. Navale, S. Navale, M. Chougule, S. Ingole, F. Stadler, R. Mane, Mu. Naushad, Patil, V. *Journal of Colloid and Interface Science.* 2017, **487**, 458–464.

29. S. Navale, V. Mali, S. Pawar, R. Mane, M. Naushad, F. Stadler, V. Patil, *RSC Adv.,* 2015, **5**, 51961-51965.

30. A. Vinu, D. Sawant, K. Ariga, M. Hartmann, S. Halligudi, *Microporous Mesoporous Mater.,* 2005, **80**, 195.

31. V. Kumar, S. Chatterjee, P. Sharma, S. Chakrabarty, Chilukuri, V. Avadhani, S. Sivaram, J. Polym. Sci. Part A. 2018, **56**, 1046-1057.

32. H. Yu, M. C. Tian Shen, Z. Wang, *Polym. Chem.* 2013, **4**, 961.

33. M. Mara, Aleksic, Pantic Jelena, P. Vera, Kapetanovic, *Physics, Chemistry and Technology*, 2014, **12**, 55- 63.

34. S. Mohapatra, A. Acharya, G. S. Roy, *Lat. Am. J. Phys. Educ.,* 2012, **6**, 380.

35. J. Smithyman, Q. H. Do, C. Zeng, Z. Liang, *J. Power Sources,* 2015, **277**, 59-63.

View Article Online
DOI: 10.1039/C9NJ02877C

36. R. Kotz, M. Carlen, *Electrochem. Acta.* 1999, **45**, 2483-2498.

37. I. Dhole, S. Navale, Y. Navale, Y. Jadav, C. Pawer, S. Suryavanshi, V. Patil, *J. Mater Sci: Mater Electron.* 2017, **28**,10819–10829.

38. B. Conway, Electrochemical supercapacitors: Scientific fundamentals and technological applications. *Kluwer, New York*, 1999.

39. M. Stoller, S. Park, Y. Zhu, J. An, R. S. Ruoff, *Nano letters,* 2008, **8**, 3498-3502.

40. Z. Gao, F. Wang, J. Chang, D. Wu, X. Wang, z. Xu, S. Gao, K. Jiang, *Electrochimica Acta,* 2014, **133**,325–334.

41. S. Mujawar, S. Ambade, T. Battumur, R. Ambade, S. Lee, *Electrochimica Acta,* 2011, **56**, 4462-4466.

42. J. Bockris, B. Conway, R. White, *Modern Aspects of Electrochemistry No 14; Plenum Press: New York, NY, USA,* 1982; Chapter 2.

43. J. Harris, P. DeRose, M. Bruening, *J. Am. Chem. Soc.,* 1999, **121**, 1978–1979.

44. P. Sen, A. De, *Electrochimica Acta,* 2010, **55**, 4677–4684.

45. B. Vidhyadharan, et al. *J. Mater. Chem. A* 2014, **2**, 6578–6588.

46. W. Sun, X. Rui, M. Ulaganathan, S. Madhavi, Q. Yan, *J. Power Sources,* 2015, **295**, 323-328.

47. a) C. R. Deblase, K. E. Silberstein, T. T. Truong, H. D. Abrun, W. R. Dichtel, *J. Am. Chem. Soc.* 2013, **135**, 16821-16824.
b) S. Chai, N. Hu, Y., Han, X. Zhang, Z. Yang, L. Wei, H. Wei, *RSC Adv.* 2016, **6**, 49425-49428.

48. F. Xu, S. Jin, H. Zhong, D. Wu, X. Yang, X. Chen, H. Wei, R. Fu, D. Jiang, Scientific Rep., 2015, **5**, 8225.

49. V. H. Pham, T. Gebre, J. H. Dickerson, *Nanoscale.*, 2015, **7**, 5947-5950.

50. X. Liu, L. Zhou, Y. Zhao, L. Bian, X. Feng, Q. Pu, *ACS Appl. Mater. Interfaces.*, 2013, **5**, 10280-10287

51. A. Amali, J. Sun, Q. Xu, *Chem. Commun.,* 2014, **50**, 1519.

52. D. Puthusseri, V. Aravindan, S. Madhavi, S. Ogale, *Energy Environ. Sci.,* 2014, **7**, 728-735.

53. N. Wickramaratne, J. Xu, M. Wang, L. Zhu, L. Dai, M. Jaroniec, *Chem.Mater.* 2014, **26**, 2820-2828.

54. S. Yang, Y. Lin, X. Song, P. Zhang, L. Gao, *ACS Appl. Mater. Interfaces.*, 2015, **7**, 17884-17892.

55. K. L. Zhang, Zhang, X. Zhao, Wu, *J. Chem. Mater.* 2010, **22**, 1392-1401.

56. L. Li, Z. A. Hu, N. An, Y. Y. Yang, Z. M. Li, H. Y. Wu, *J. Phys. Chem. C*. 2014, 118, 22865-22872.